18th IFHTSE CONGRESS
International Federation for Heat Treatment and Surface Engineering
IFHTSE
ANAIS
PROCEEDINGS
ISSN 1516-392X

EFFECT OF THE HYDRODYNAMIC CONDITIONS ON THE VAPOR FILM DURING FORCED CONVECTIVE QUENCHING[1]

H.J. Vergara Hernández[2]
B. Hernández Morales[3]
G. Solorio Diaz[4]
G.Gutiérrez-Gnechi[2]

Abstract
To achieve the high cooling rates required during quenching processes, the parts are quenched in agitated liquid baths which modifies boiling phenomena at the part-fluid interface and, therefore, the thermal field evolution within the part. In spite of this, the interactions between fluid hydrodynamics and wetting front kinematics have not been investigated in detail. In this paper we studied the effect of vorticity and pressure gradients near the part surface on wetting front kinematics during forced convective quenching by means of a mathematical model which couples the velocity, thermal and phase fraction fields. The particular physical condition studied was that of water at 60°C flowing parallel to a flat-end cylindrical stainless steel probe, for which experimental results were already available. The computed pressure and vorticity fields show larger gradients near the probe end as the fluid velocity increases. This behavior favors a thicker vapor film near the probe base reducing heat transfer to the quenching bath locally. In contrast, low pressure and vorticity gradients occurring for low fluid velocities favor a uniform vapor film. A direct consequence of the non-uniform vapor film thickness occurring at high velocities is a significant thermal gradient along the probe axis which favors distortion.
Keywords: Wetting front; Forced convective quenching; Modeling.

[1] *Technical contribution to the 18th IFHTSE Congress - International Federation for Heat Treatment and Surface Engineering, 2010 July 26-30th, Rio de Janeiro, RJ, Brazil.*
[2] *Posgrado de Ciencias en Metalurgia, Instituto Tecnológico de Morelia, Av. Tecnológico # 1500, Colonia Lomas de Santiaguito, Morelia, Michoacán, 58120.*
[3] *Depto. de Ingeniería Metalúrgica, Facultad de Química, Universidad Nacional Autónoma de México, Cd. Universitaria, México, D.F., 04510.*
[4] *Facultad de Ingeniería Mecánica, UMSNH, Santiago Tapia 403, Centro, Morelia, Michoacán, 58000.*

INTRODUCTION

The evolution of the thermal field during quenching dictates the final properties produced in the quenched part. To achieve the high cooling rates required during the process, the parts are usually quenched in agitated liquid baths at temperatures well below the liquid saturation temperature. The latter generates a sequence of boiling phenomena at the part/quench bath interface as follows:[1] initially, a vapor film surrounds the metallic part; as cooling progresses, the vapor film thickness decreases until it breaks down and is substituted by bubbles; after a period of rapid bubble formation bubbling diminishes progressively until it completely ceases and heat transfer occurs by pure convection. During quenching, the kinematics of the wetting front, which is defined as the loci of the boundary between the vapor film and the occurrence of bubbles, is of outmost importance. When quenching in water, the wetting front advances slowly while an explosive behavior has been observed for polymeric quench baths. Boiling phenomena during quenching do not occur isolated from the events taking place within the quench bath, i.e., the velocity, pressure and vorticity fields in the neighborhood of the quenched part may affect them which in turn would modify the kinematics of the wetting front.

Tensi et al.[2] studied boiling phenomena during quenching using flat-end cylindrical probes (15 mm-dia. x 100 mm-long) heated up to 950°C and cooled in still water. The occurrence of the boiling stages described above was characterized by measuring the electrical conductivity between the probe and the quench tank. Due to the insulating effect of the vapor film, which is stable at high temperatures, electrical continuity is very por under those conditions. As the vapor film starts to collapse at any given point on the probe surface, the electrical conductivity increased proportionally to the surface area where nucleate boiling was taking place.

Künzel at al.[3] also used flat-end cylindrical probes –made with Cr-Ni alloys – to study boiling phenomena during the quench. They reported that the collapse of the vapor film started at the base of the probe and continued moving upwards. This moving boundary, that separates film boiling from transition boiling, is also known as the wetting front.

Recently developed quench processes[4,5] have prompted the design of experiments[6,7] aimed at quantifying the kinematics of the wetting front as precisely as possible in order to understand fully the interaction between the probe surface and the hydrodynamics of the quench bath with the ultimate goal of improving industrial processes. For example, Vergara-Hernández and Hernández-Morales[7] developed a specially designed apparatus and used a conical-end cylindrical probe to study the kinematics of the wetting front at the high fluid velocities usually encountered in industrial operations. In their study, they included flat-end probes also. The commonly-used flat-end probes showed a chaotic collapse of the vapor film near the probe base while the conical-end probes allowed a uniform and stable advance of the wetting front. Also, the flat-end probes showed a non-uniform vapor film thickness; particularly, a considerably thicker vapor film was observed near the base of the probe.

Without a clear understanding of the phenomena at the part-fluid interface the operating conditions may be incorrectly set which would provoke a non- uniform heat extraction pattern increasing the probability of part distortion and even fracture. Thus, the objective of this work is to develop a mathematical model to simulate the hydrodynamic and thermal phenomena occurring near the base of the flat-end cylindrical probes to understand the physical phenomena responsible for the

observed behavior in the set of previous experiments. Given that a phase change (from liquid to vapor) also occurs, it is necessary to include a mass transfer model.

PREVIOUS EXPERIMENTAL WORK

Wetting front kinematics during forced convective quenching of flat-end cylindrical probes (12.7 mm-dia. x 50 mm long) cooled with water at 60ºC flowing vertically within a plexiglass tube (44 mm I.D. x 170 mm long) was characterized experimentally by measuring the thermal response within the probe along its longitudinal axis and video-recording the events at the surface probe. Experimental details are given elsewhere;[7] thus only relevant points will be mentioned here. A desirable experimental condition when working with forced convective flows is that of a fully developed flow; this condition usually implies that a large test section must be employed. Additionally, the probe must have a short travel within the fluid to avoid excessive cooling. Using particle image velocimetry (PIV) measurements and computational fluid dynamics (CFD) results the minimum length of plexiglass tube required was determined. The probe was heated to 915°C in an electrical resistance furnace, the water flow was steadied and then the probe was quickly immersed in the flowing water. The probe was machined from AISI 304 stainless steel stock bar and was instrumented with four 1/16 in. dia, inconel sheathed, type-K thermocouples. The thermal response was recorded using a computer-controlled data acquisition system and at the same time the events taking place at the probe surface were video-recorded. Two free-stream water velocities were studied: 0.2 and 0.6 m/s.

From the video-recordings, several images were obtained. In Figure 1, four images corresponding to times between 0.2 and 15 seconds after the start of quenching the stainless steel probe in water at 60°C flowing at 0.20 m/s are shown. In Figure 1a it can be observed that, 0.2 s after the start of the quench, the surface probe temperature is high enough to vaporize the liquid near the probe forming a stable vapor film around it. When the probe temperature falls below the Leidenfrost temperature the vapor film collapses and nucleate boiling start (see Figure 1b) which leads to the occurrence of the wetting front. As the cooling progresses further the surface temperature falls below the liquid saturation temperature and the cooling occurs by pure convection. From the images it is clear that the wetting front advances in a non-symmetrical fashion.

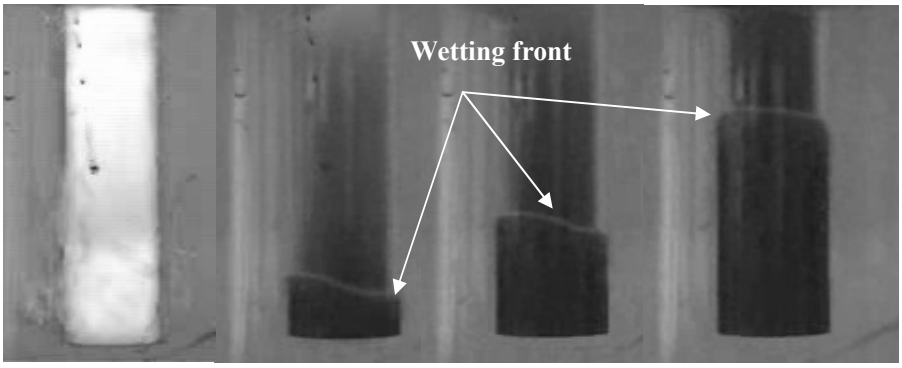

(a) (b) (c) (d)

Figure 1. Sequence of events at the probe surface for an experiment with water at 60°C flowing at 0.2 m/s: (a) 0.2 s, (b) 7.5 s, (c) 9.2 s y d) 15 s, after the probe, initially at 915°C, was immersed in the quench bath.[7]

Figure 2 shows four images corresponding to the probe quenched in water at 60°C flowing at 0.6 m/s. During the first few seconds during the quench an 18 mm-long region near the probe base shows a thicker vapor film (Figures 2a and 2b). As a consequence heat extraction in that region diminishes and a significant and non-uniform longitudinal thermal gradient occurs (Figure 2b). As the process advances the vapor film collapses near the probe base (Figure 2c) but, in comparison with the lower fluid velocity experiment the wetting front advances in a more chaotic fashion. The non-uniform thermal gradient may cause distortion in the quenched part.

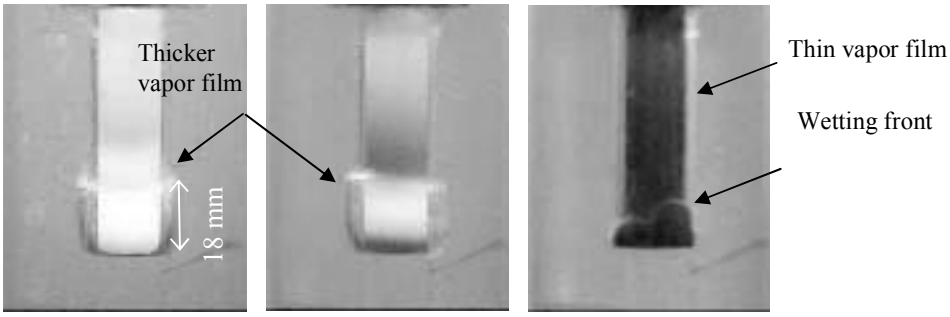

Figure 2. Sequence of events at the probe surface for an experiment with water at 60°C flowing at 0.6 m/s: (a) 0.46 s, (b) 3.0 s and (c) 7.4 s after the probe, initially at 915°C, was immersed in the quench bath.[7]

MATHEMATICAL MODEL

A fundamental problem regarding the computational simulation of boiling phenomena lies in the description of the liquid/vapor interface under unsteady state conditions which in the past led to a number of simplifications. For example Lee and Nydahl[8] performed a numerical simulation of the nucleation of a bubble at a wall assuming a perfectly spherical shape. Welch[9] could simulate a deformable bubble using a specially designed triangular mesh in 2D. However, Welch as well as Son and Dhir[10] could only simulate few seconds of the process due to mesh distortion. Juric and Triggvason[10] developed a front-tracking method to remove difficulties associated with a completely deformable interface. Using this methodology, other investigations on the formation and collapse of vapor films in pool boiling (see, for example[11]) could be developed.

Modeling of boiling phenomena in CFD codes is based on one or more surfaces to separate the liquid and vapor phases.[12] They may be classified in two groups: 1) the two fluids are considered immiscible (VOF techniques) and 2) the two fluids are allowed to mix (MIXTURE techniques). In this work we developed the mathematical model using the MIXTURE model, implemented in the commercially-available CFD code Fluent.[13]

The model includes the continuity, momentum conservation and energy conservation equations for the mixture introducing the mixture density (ρ_m), velocity (u_m) and viscosity (μ_m), plus the liquid (α_l) and vapor (α_v) mass fractions:

$$\frac{\partial}{\partial t}(\rho_m) + \nabla \cdot (\rho_m \vec{u}_m) = 0 \qquad (1)$$

$$\frac{\partial}{\partial t}(\rho_m \vec{u}_m) + \nabla \cdot (\rho_m \vec{u}_m \vec{u}_m) = -\nabla p + \nabla \cdot [\mu_m (\nabla \vec{u}_m + \nabla \vec{u}_m^T)] + \rho_m \vec{g} + \vec{F} + \nabla \cdot \left(\sum_{k=1}^{n} \alpha_k \rho_k \vec{u}_{dr,k} \vec{u}_{dr,k} \right) \quad (2)$$

$$\frac{\partial}{\partial t} \sum_{k=1}^{n} (\alpha_k \rho_k E_k) + \nabla \cdot \sum_{k=1}^{n} (\alpha_k \vec{u}_k (\rho_k E_k + p)) = \nabla \cdot (k_{eff} \nabla T) + S_E \quad (3)$$

$$1 = \alpha_l + \alpha_v \quad (4)$$

$$\rho_m = \alpha_l \rho_l + \alpha_v \rho_v \quad (5)$$

$$u_m = \frac{\alpha_l \rho_l u_l + \alpha_v \rho_v u_v}{\rho_m} \quad (6)$$

$$\mu_m = \alpha_l \mu_l + \alpha_v \mu_v \quad (7)$$

The conservation equations are written for a turbulent, unsteady-state flow. The heat source term (S_E) in equation (3) was introduced to the CFD code through a user- defined function according to:

$$S_E = \frac{1}{\Delta}\left[k_v\left(T_v - T_{sat}\right) - k_l\left(T_{sat} - T_l\right)\right] \quad (8)$$

Where T_v y T_l are the vapor and liquid temperatures near the interface, T_{sat} represents the interface temperature and Δ is a distance within the vapor or liquid phase; according to Esmaeeli and Tryggvason[11] $h \le \Delta \le 2h$ where *h* is the grid spacing.

The $k-\varepsilon$ [13] model was used to describe the turbulent characteristics of the flow:

$$k = \frac{3}{2}(u_{avg} I)^2 \quad (9)$$

$$I = 0.16(\mathrm{Re}_{D_H})^{-1/8} \quad (10)$$

$$\varepsilon = C_\mu^{3/4} \frac{k^{3/2}}{\ell} \quad (11)$$

I is the turbulent intensity, u_{avg} is the fluid average velocity, is Re_{D_H} the Reynolds Lumber based on the hydraulic diameter, ℓ is the length of the turbulent scale (ℓ = 0.07 L), L is duct the diameter and C_μ is a constant (0.09).

An experimentally determined velocity profile was applied as the inlet boundary condition.[7] This profile can be represented by:

$$u(r) = \left[\frac{(0.2389\text{E-}06 + |\mathrm{r}|)}{(0.6791\text{E-}03 + 1.007 \cdot |\mathrm{r}|)} + 7.131 \cdot |\mathrm{r}| \right] u_{avg} \qquad -R < r < R \quad (12)$$

where $u(r)$ is the inlet velocity at a given radial position, u_{avg} is the average velocity, r is the radial position measured from the tube center and R is the tube radius.

In the model, the outlet surface was drawn normal to the longitudinal axis of the probe and located at the top surface of the probe; the velocity gradients, in the flow direction, were set to zero at the outlet surface. As it is customary, the velocity at all fluid/solid boundaries was set to zero. The computational model is shown in Figure 4.

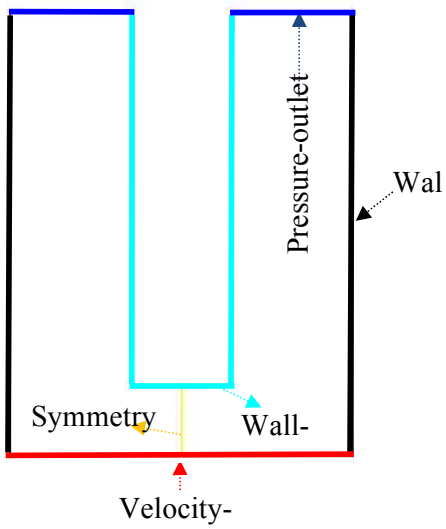

Figure 4. The computational model used to represent the system.

RESULTS

Figures 5 and 6 show streamlines and static pressure distribution for both water velocities studied. In Figure 5 it can be appreciated that at the probe base a stagnant region ($\vec{v}$ = 0) occurs. Also, some of the streamlines coincide with the vertex of the probe base producing a local jump in the velocity field and, consequently, a lower static pressure in that zone.

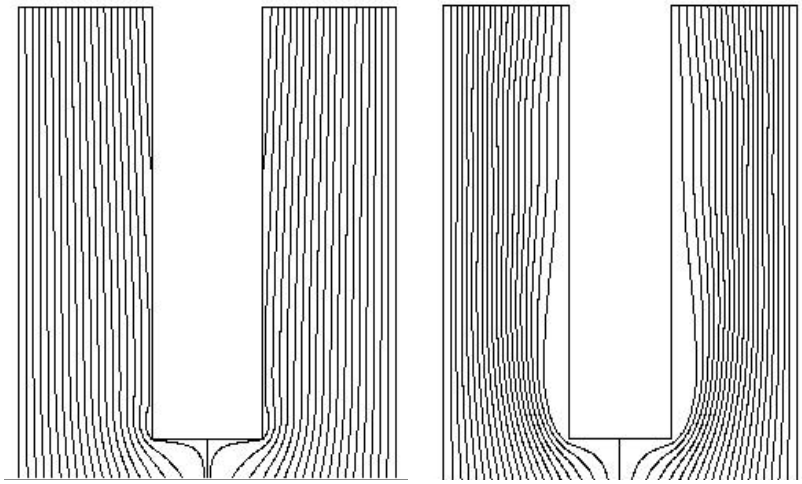

(a) (b)

Figura 5. Streamlines around the probe quenched in water at 60°C flowing at: (a) 0.20 m/s y (b) 0.60 m/s. The images correspond to 0.1 s after start of quenching.

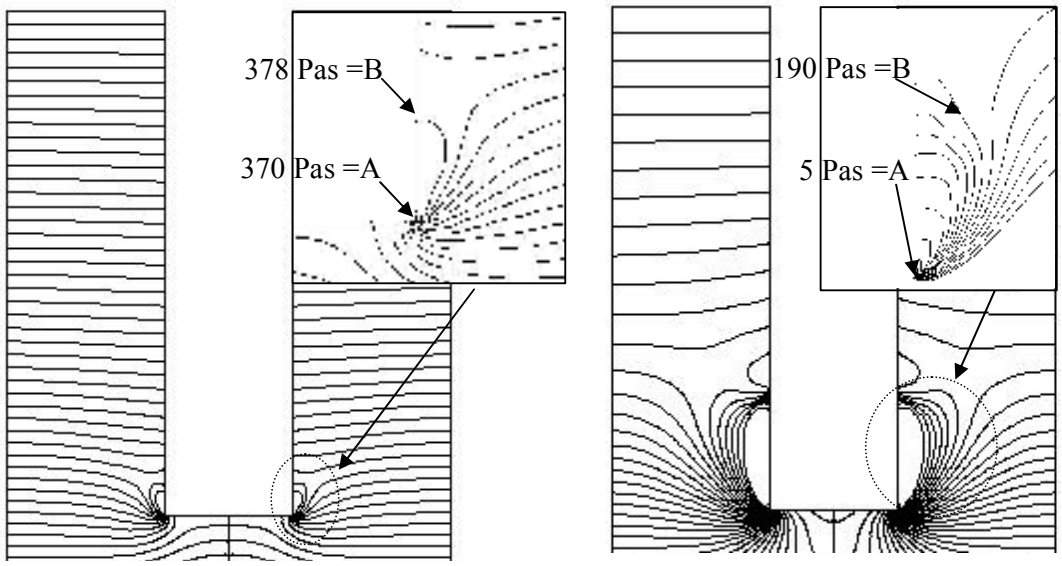

Figure 6. Contours of static pressure for the probe quenched in water at 60°C flowing at: (a) 0.20 m/s y (b) 0.60 m/s. The images correspond to 0.1 s after start of quenching.

Given that the static pressure is higher at point B of Figure 6a than at point A, a backflow within the boundary layer is produced (see Figure 7).

Thus, the sharp corner at the probe base results in a change of direction of the fluid flow which prompts the boundary layer separation. When the fluid flows at 0.6 m/s, the pressure gradient increases significantly (see Figure 6b) and the vapor film finds the conditions needed to expand.

Figure 8 shows the vorticity field near the probe base. The vorticiy gradient is larger and expands trough a larger region for the high fluid velocity.

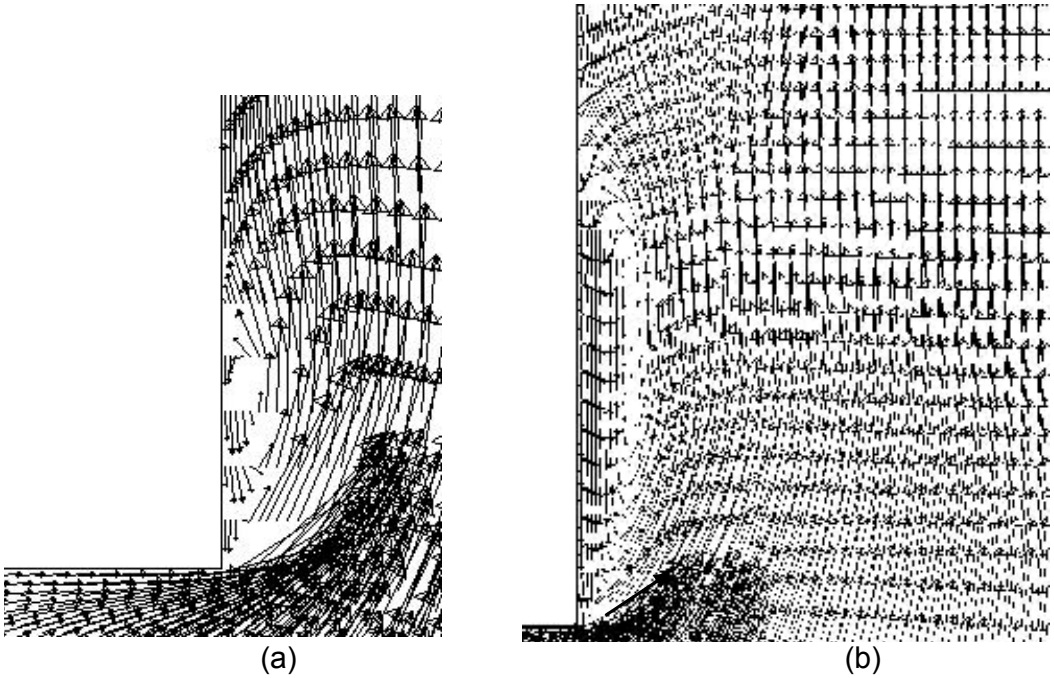

Figure 7. Velocity field near the probe base for water at 60°C flowing at: (a) 0.2 m/s and (b) 0.6 m/s. Note the Boundary layer separation and backflow. The images correspond to 0.1 s after start of quenching.

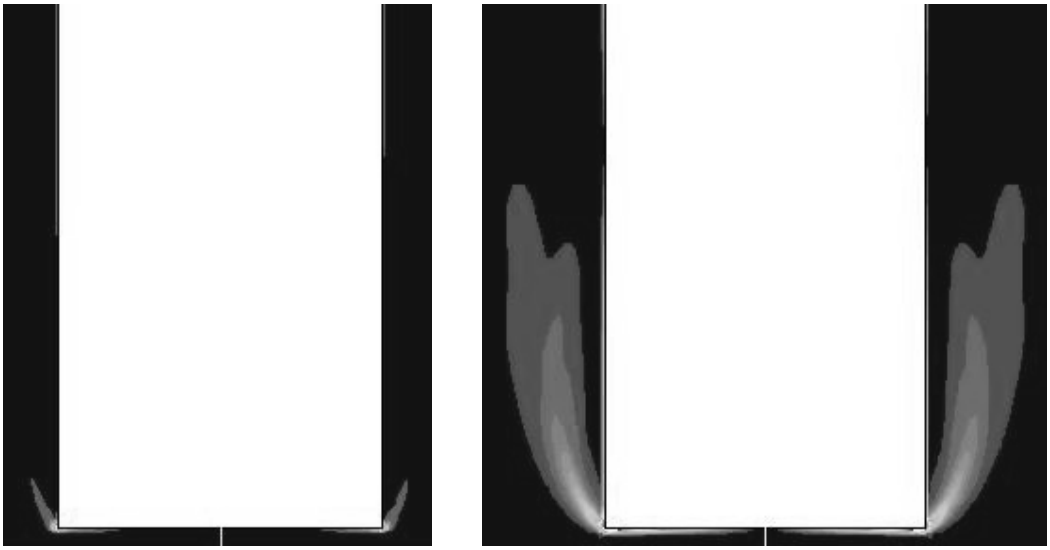

(a) (b)

Figure 8. Vorticity contour maps (1/s) computed for water at 60 ºC flowing at: (a) 0.20 and (b) 0.60 m/s, in the neighborhood of a flat-end cylindrical probe. The images correspond to 0.1 s after start of quenching.

The vapor film thickness computed with the model is shown in Figure 9 for both liquid velocities. As can be seen in Figure 9a, the vapor film thickness for low fluid velocity is fairly uniform round the probe which was observed experimentally (see Figure 1a. when the water velocity increases up to 0.6 m/s a 15 mm-long region at the probe base shows a thicker vapor film which is similar both in shape and length to the one recorded in the experiments (see Figures 2a and b). These observations validate the mathematical model used in this work.

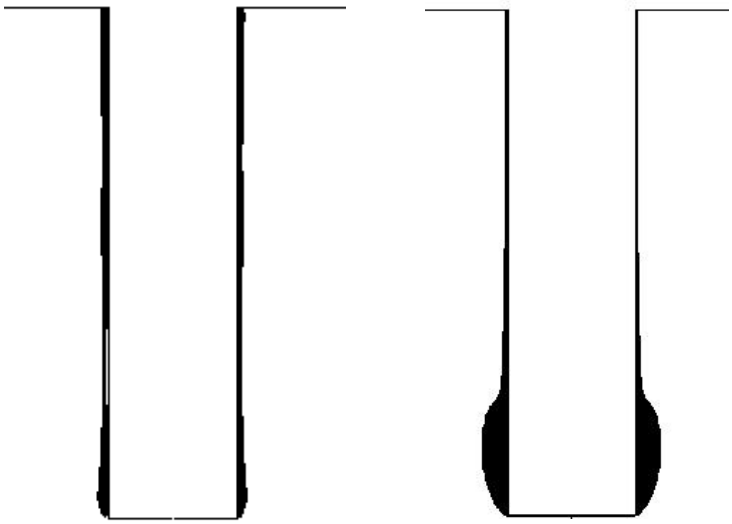

(a) (b)

Figure 9. Phase fraction around the probe quenched in water at 60°C flowing in water at: (a) 0.20 m/s y (b) 0.60 m/s. Vapor phase (black) and liquid phase (white). The images correspond to 0.1 s after start of quenching.

CONCLUSIONS

Boiling events at the part/liquid interface in quenching processes are modified by the characteristics of the flow field around the part. In particular, sharp corners in quenched parts produce changes in the liquid velocity direction which favor local pressure losses, boundary layer separation and high vorticity gradients. These effects favor the expansion of the vapor film which in turn promotes large, non-uniform thermal gradients in the part which may cause distortion.

REFERENCES

1 Totten, G.E., Bates, C.E., and Clinton, N.A., 1993, Handbook of Quenchants and Quenching Technology, ASM International, Materials Park, OH.
2 Tensi, H.M., and Stitzelberger, J., 1988, “Influence of wetting kinematics on quenching and hardening in water based polymers with forced convection”, Proc. Heat Treatment and Surface Engineering – New Technology and Practical Applications, Chicago, Illinois, USA, pp. 171–176.
3 Kunzel, T.H., Tensi, H.M., and Welzel, G., 1986 “Rewetting rate – the decisive characteristic of a quenchant”, Proc. 5th International Congress on Heat Treatment of Materials, Budapest-Hungary, pp.1806–1813.
4 Totten, G.E., Kobasko,N.I., Aronov, M.A., and Powell, J., 2002, “Overview of Intensive-Quenching Processes”, Industrial Heating 69 (4), pp. 31–33.
5 Kobasko, N.I., 2002, “Quenching Apparatus and Method For Hardening Steel Parts”, USP 6,364,974.
6 Kobasko, N.I., and Guseynov, Sh.E., 2008, “Initial heat flux densities and duration of non-stationary nucleate boiling during quenching”, Proc. of the 5th WSEAS International Conference on Heat and Mass Transfer, J. Krope et al., eds., Acapulco, Mexico, pp. 104–109.
7 Vergara-Hernández, H.J., and Hernández-Morales, B., 2009, “A novel probe design to study wetting front kinematics during forced convective quenching” Experimental Thermal and Fluid Science, 33, pp. 797–807.
8 Lee, R.C., and Nydahl, J.E., 1989, “Numerical calculations of bubble growth in nucleate boiling from inception through departure”, ASME Journal of Heat Transfer, 111, pp. 474–479.
9 Welch, S.W.J., 1995, “Local simulation of two-phase flows including interface tracking with mass transfer”, Journal of Computational Physics, 121, pp. 142–154.
10 Juric, D., and Tryggvason, G., 1998, “Computations of boiling flows”, International Journal of multiphase flow, 24, pp. 387–410.
11 Esmaeeli, A., and Tryggvason, G., 2004, “Computations of film boiling-Part I: numerical method”, International J. of Heat and Mass Transfer, 47,pp. 5451–5461.
12 Ait, Y., 2005, “Physical modeling of leading edge cavitation: Computational methodologies and applications to hydraulic machinery”, Ph.D. thesis, Ecole Polytechnique Fédérale de Lausanne, Switzerland.
13 http://www.fluent.com/.